Materials Science-Poland, *Vol. 26*, *No. 4*, *2008*

Micromagnetic properties of Co/Pt multilayers deposited on various buffer layers

M. CZAPKIEWICZ[1*], J. KANAK[1], T. STOBIECKI[1], M. KACHEL[1], M. ŻOŁĄDŹ[1], I. SVEKLO[2], A. MAZIEWSKI[2], S. VAN DIJKEN[3]

[1]Department of Electronics, AGH University of Science and Technology, al. Mickiewicza 30, 30-059 Cracow, Poland

[2]Institute of Experimental Physics, University of Bialystok, Lipowa 41, 15-424 Bialystok, Poland

[3]VTT Micro and Nanoelectronics, P.O. Box 1000, FI-02044 VTT, Finland

A study on the buffer layer dependence of the film texture, surface roughness, and magnetization reversal process in Co/Pt multilayers prepared by dc magnetron sputtering is presented. Oxidized Si(100) wafer was covered with four different buffers: (A) 10 nm Cu, (B) 5 nm Ta/10 nm Cu, (C) 5 nm Ta/10 nm Cu/5 nm Ta, and (D) 5 nm Ta/10 nm Cu/5 nm Ta/10 nm Cu. The growth of [2 nm Pt/0.5 nm Co]×5/2 nm Pt on top of these buffer layers results in a large variation in the *fcc* (111) Co/Pt texture and surface morphology. All films have the perpendicular magnetic anisotropy but magnetization reversal process, studied by the magnetooptic Kerr effect (MOKE) and magnetic force spectroscopy (MFM), strongly depends on the buffer used. Observation of magnetic domains evolution under a MOKE microscope allows one to calculate from magnetization relaxation curves average dispersion of energy barriers of the thermal activated magnetization switching process. The application of MFM in external magnetic field allows one to follow the dynamics of direct and indirect magnetization switching procesess up to submicrometer scale.

Key words: *perpendicular anisotropy; magnetic domain; magnetization reversal*

1. Introduction

Ferromagnetic multilayers with anisotropy perpendicular to the film plane are potentially interesting for application in high density magnetic recording. Systems with two magnetic states, “up” and “down”, with a good efficiency of the polar magneto-optical Kerr effect, are thus attractive for novel memory storage devices. Perpendicular magnetic anisotropy (PMA) phenomena have been extensively investigated in mul-

*Corresponding author, e-mail: czapkiew@agh.edu.pl

tilayer films prepared by a sequential deposition of ferromagnetic metals (Co, Fe, Ni) and nonferromagnetic noble metals (Pt, Au, Pd) [1–4]. More recently, perpendicular exchange bias effects have been studied in systems consisting of a PMA stack (for example [Pd/Co]n or $[Pt/Co]_n$) and an antiferromagnetic layer (CoO [5, 6], FeMn [7, 8] or IrMn [9–11]). Many authors reported a variety of observed domain structures during magnetization reversal processes [12–14] occurring due to nucleation of a large number of small domains or by a smooth growth of a large cylindrical domains, or else by creep growth of irregular domains. A detailed study of magnetization reversal process by means of magnetooptic Kerr effect (MOKE) magnetometer, MOKE microscopy or by magnetic force microscopy (MFM) revealed that a particular domain structure and its dynamics related to the shape of the magnetization hysteresis loop depend strongly on the micromagnetic properties resulting from the layer interface structure.

In this paper, results of studies of structural, microstructural, magnetic and micromagnetic properties are reported of PMA multilayer systems of [2 nm Pt/0.5 nm Co]×5/2 nm Pt deposited on various buffer layers with different degrees of *fcc* (111) Co/Pt texture. The model of energy barriers for thermally activated magnetization reversal process, successfully used elsewhere [15, 16], reveals a distinctive correlation between spatial dispersion of energy barriers and texture of used buffer layers.

2. Experimental

The [2 nm Pt/0.5 nm Co]×5/2 nm Pt multilayers were grown on four buffers: 10 nm Cu (A), 5 nm Ta/10 nm Cu (B), 5 nm Ta/10 nm Cu/5 nm Ta (C), and 5 nm Ta/10 nm Cu/5 nm Ta/10 nm Cu (D). Recently, it was shown that for a sample with Cu buffer (sample A), a small contribution of Cu (200) texture was observed in addition to (111) texture [17]. However, a pronounced (111) Cu texture appears when Ta is used as a seed layer on silicon oxide (sample B). The buffers C and D were used to change the texture degree by repetition of Ta/Cu bilayers in the system. The buffers and Co/Pt multilayers were deposited on Si(100) wafer with 500 nm thick SiO_2 by dc magnetron sputtering at ambient temperature.

After deposition, roughness and morphology of the multilayer surfaces were examined by AFM. The structure was characterized by X-ray diffraction (XRD) using θ–2θ scans, rocking curves (ω scans) and X-ray reflectivity [11]. SQUID measurements with the field parallel to the film plane were performed to saturate the magnetization in the film plane and determine effective anisotropy field H_K. The effective anisotropy is given by the equation

$$K_{\text{eff}} = \frac{1}{2}\mu_0 H_K M_S \tag{1}$$

beings a superposition of crystalline anisotropy of Co layers and surface anisotropy of the Co/Pt interface [18]. This large effective anisotropy energy is responsible for the perpendicular to the plane orientation of magnetization in a remanent state. Magneti-

zation reversal hysteresis loops with field perpendicular to the film plane were recorded by means of the MOKE magnetometer [19] to verify the coercivity and hysteresis loop squareness. The magnetooptical contrast of magnetic domains was observed by the MOKE microscopy [20] with the spatial resolution down to 1 μm. Thanks to a special system for real-time image processing, evolution of domain structure was recorded and stored with the 25 frames per second rate. The thermally activated magnetic reversal process was studied by recording the evolution of magnetic domains in a constant field perpendicular to the film plane. It is convenient to study relaxation of metastable state of magnetization in a constant negative magnetic field lower than the critical switching field [21]. Magnetization relaxation from a saturated state M_S to $-M_S$ can be represented by the fractional magnetization $B(t)$ not yet reversed at a time t

$$B(t) = \frac{M(t) + M_S}{2M_S} \tag{2}$$

Such a fractional area B can be derived from the image of MOKE contrast as the ratio of the white area (spins down) to the total area of the observed ferromagnetic sample. For the PMA thin films and multilayers magnetization reversal occurs usually by nucleation and growth of cylindrical domains. As was shown by Labrune et. al. [22], the Fatuzzo model [23] can be used to express the influence of competition between the nucleation probability rate R and domain expansion velocity v on the shape of $B(t)$ by a dimensionless parameter

$$k = \frac{v}{r_c R} \tag{3}$$

where r_c is the radius of the initial domain. The nucleation probability rate as well as the velocity of domain expansion depend exponentially on the activation energy barrier W

$$R = R_0 \exp\left(-\frac{W - \mu_0 M_S H V_B}{k_B T}\right) \tag{4}$$

$$v = v_0 \exp\left(-\frac{W - \mu_0 M_S H V_B}{k_B T}\right) \tag{5}$$

The energy barrier decreases with the external magnetic field H proportionally to the Barkhausen volume V_B, i.e. magnetization volume that reverses during a single activation event. Under the above assumptions, the relaxation of magnetization is given by the Fatuzzo formula:

$$B(t) = \exp\left(-2k^2\left(1 - \left(Rt + k^{-1}\right) + 0.5\left(Rt + k^{-1}\right)^2 - \mathrm{e}^{-Rt}\left(1 - k^{-1}\right) - 0.5k^{-2}\left(1 - Rt\right)\right)\right) \tag{6}$$

The shape of above function, plotted against reduced time t/t_{50}, depends on the parameter k [22]. A high k parameter ($k >> 10$, magnetization relaxation driven by domain growth) is responsible for a Gaussian shape of relaxation; a low k parameter ($k << 1$, magnetization relaxation driven by domain nucleation) generates an exponential relaxation shape (Fig. 1). Parameters R, derived from the fitting procedure of the Fatuzzo model to experimental data recorded for various fields H, can be used to estimate the average V_B value from the slope of the plot ln(R) vs. H (Eq. (4)). The Barkhausen volume can be estimated also from the plot ln(v) vs. H (Eq. (5)) if the magnetization reversal occurs by a large domains growth. The domain growth velocity can be calculated directly from the MOKE images sequence.

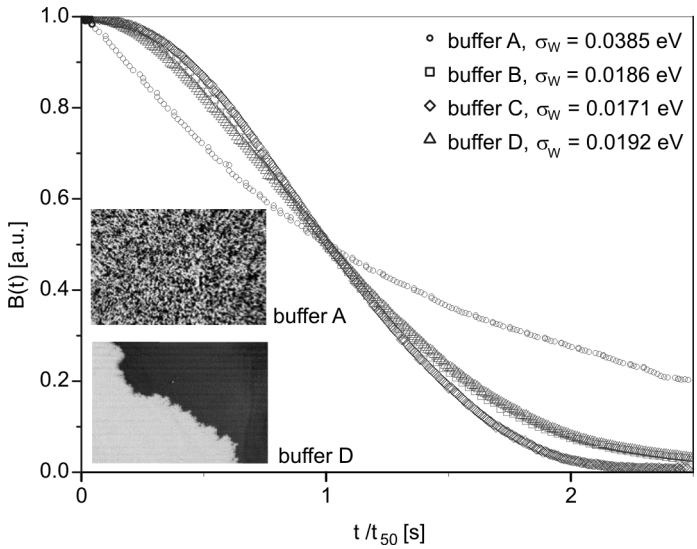

Fig. 1. Magnetization relaxation curves, derived from sequences of MOKE domain images, plotted against reduced time, with dispersions of energy barriers for thermal activated magnetization reversal process as a result. Inset: examples of MOKE images (200 μm width)

The shape of the magnetization relaxation $B(t)$ can be used also to estimate the average spatial dispersion of energy barriers of a sample, as was shown by Bruno et al. [24] under the assumption of mean energy barrier W with a square distribution of σ_W, which is reciprocal to the maximum slope of the fractional area of magnetization B plotted in function of ln(t):

$$\frac{dB}{d\ln(t)} = -\frac{k_B T}{2\sigma_W} \tag{7}$$

The above model is very convenient for interpretation of the observed domain structures. Magnetic inhomogeneities represented by average dispersion of energy barriers can be also observed during the so called indirect remagnetization process. This process occurs when an opposite field is suddenly applied during magnetization

relaxation. In this case, a new magnetization relaxation process is commencing, however from a state far from the saturation. Some papers show [25, 26] that the indirect remagnetization process is very fast compared to the initial direct magnetization relaxation, and the domain structure appears to be dendritic or hollow (so called "Swiss cheese" domains, Fig. 2).

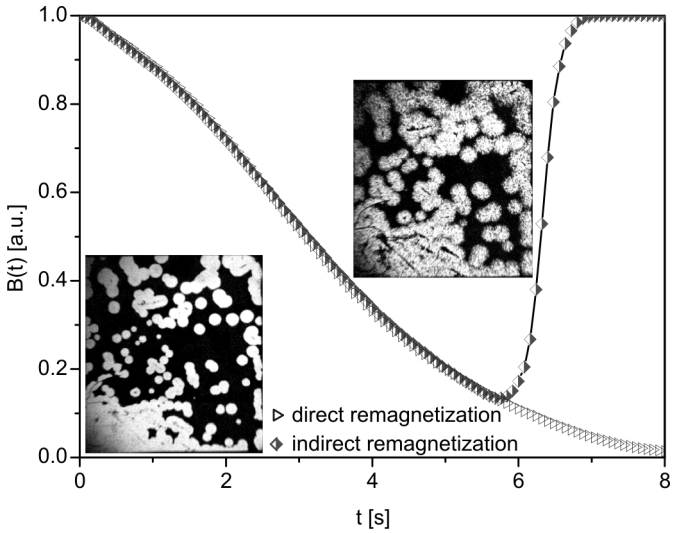

Fig. 2. Magnetization relaxation of the sample with buffer B, with a negative field constant from the saturated state (direct remagnetization) and with switching field from a negative value to a positive one in a non-saturated state (indirect remagnetization). Insets: MOKE contrast of magnetic domains (whole sample 10 mm width) before and after switching field

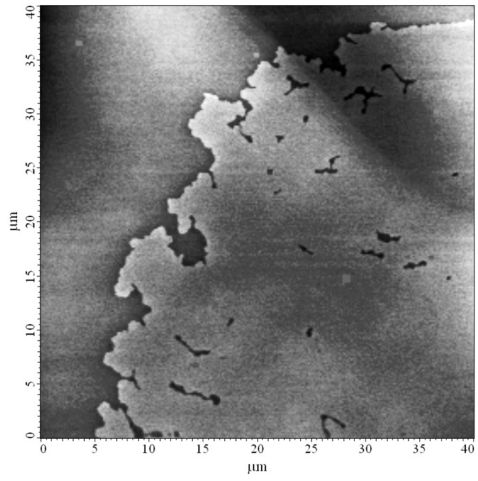

Fig. 3. MFM image of the sample D shows not yet reversed black remnants in a large white domain

This is explained by a large number of small, not reversed areas existing inside the domain, due to inhomogeneities of local magnetic properties (e.g., fluctuations of coercivity or magnetostatic dipole interactions induced by roughness [27, 28]).

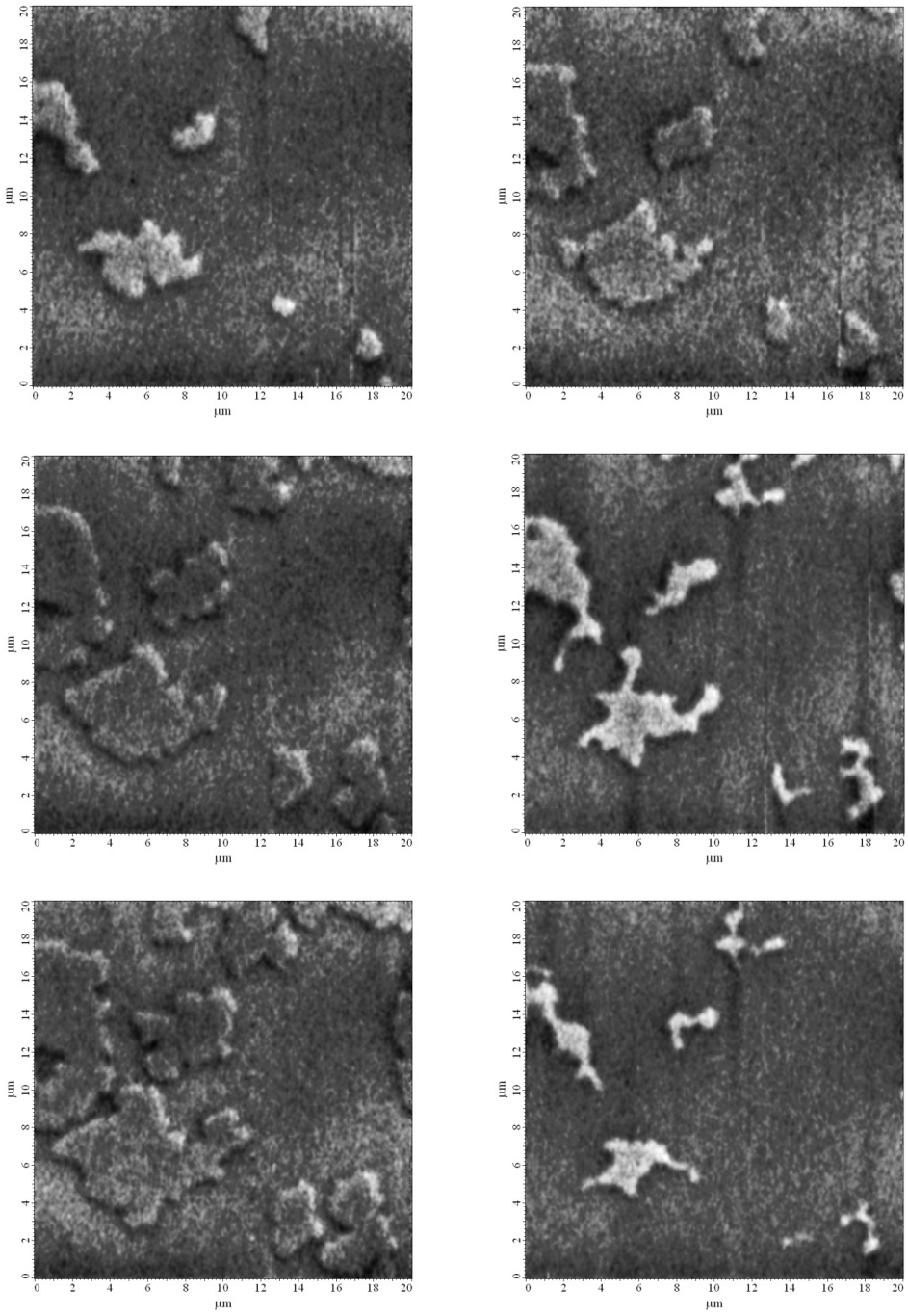

Fig. 4. Evolution of the MFM images of sample B after four pulses of 32 mT magnetic field (a–d) and after two pulses of –32 mT magnetic field (e, f). Duration of each pulse is 2 s

Sizes of these not reversed remnants are usually beyond the optical resolution of a MOKE microscope, but their existence was confirmed by the MFM images (Fig. 3). Apart from remnants inside a domain, irregularity of domain wall accounts for many centres of new domain nucleation during an indirect remagnetization process. Figure 4 shows MFM images of the domain dilation during direct relaxation and erosion of the domain during an indirect relaxation process. Each image was scanned in a zero field after 2 s pulse of a magnetic field applied perpendicular to the film plane.

3. Results

Magnetizations of the reversal hysteresis loops measured by the MOKE magnetometry are shown in Fig. 5. The hysteresis loops of highly textured samples B, C and D reveal high squareness. Excluding sample A, the highest coercivity is observed for the sample with buffer D, the lowest for the sample with buffer C. Critical switching

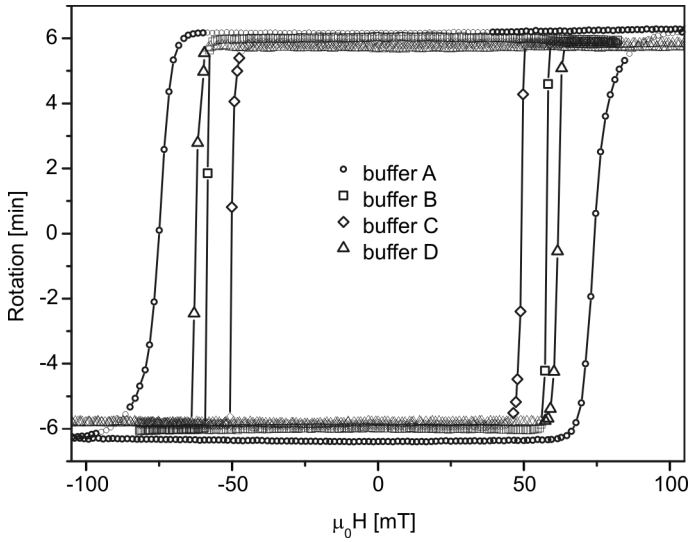

Fig. 5. MOKE hysteresis loops recorded in magnetic field with 4.5 mT/s sweeping rate

Table 1. Coercivity, effective anisotropy, Barkhausen volumes, energy dispersion and texture degree for [Pt/Co]×5 multilayers deposited at four various seed buffers

Buffer	A	B	C	D
$\mu_0 H_C$ [mT]	66.12	52.41	46.54	53.19
K_{eff} [kJ·m^{-3}]	446	921	894	931
V_B [nm^3]	1230	1310	1430	1370
σ_W [eV]	0.0385	0.0186	0.0171	0.0192
$1/2\sigma$ [deg^{-1}]	0.04	0.22	0.17	0.23

fields H_C are collected in Table 1, as well as the effective anisotropy K_{eff} derived from SQUID measurements of the in-plane magnetization. Additionally, the Barkhausen volumes V_B, calculated from Eqs. (4) and (5), have been given. The diameter of the average Barkhausen volume is close to the surface waviness length visible on the AFM scans (Fig. 6). The RMS roughness of the top surface for the used buffers is as follows: A – 0.76 nm, B – 0.52 nm, C – 0.56 nm and D – 0.92 nm.

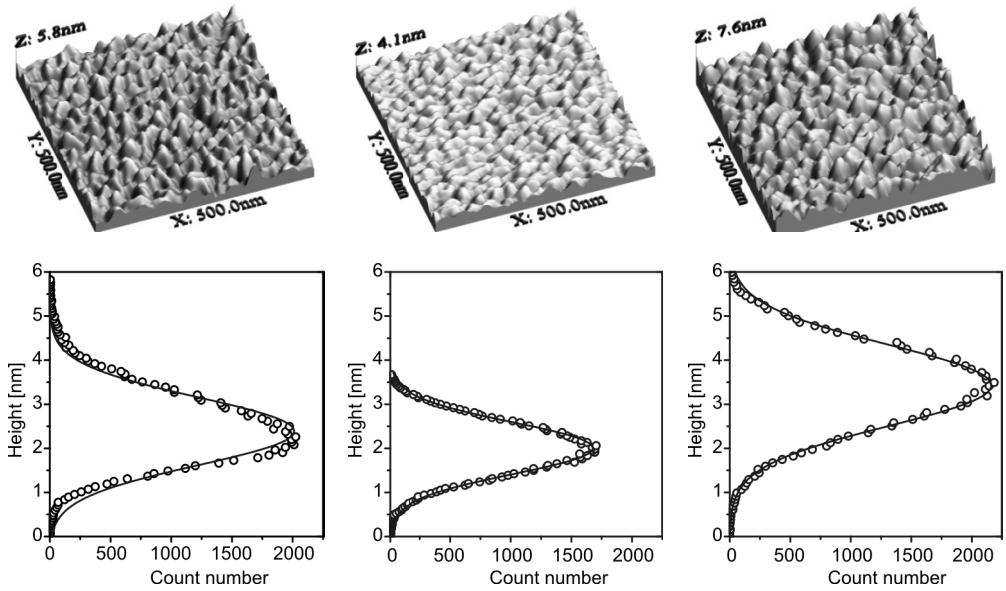

Fig. 6. Examples of AFM images of roughness on the top surface of samples A, C and D and corresponding height distributions with the Gaussian fits

The XRD θ–2θ profiles (Fig. 7) reveal very weak (111) Co/Pt superlattice peaks for the sample with buffer A and strong peaks for the B, C and D buffers. Rocking curves of (111) Co/Pt diffraction peak (Fig. 8) show that, apart from the sample with buffer A, sample D has the highest texture degree (its measure being $1/2\sigma$) and sample C has the lowest one. These results (Table 1) stand in a very good coincidence with the average spatial dispersion of energy barriers σ_W, calculated from Eq. (7). For samples with buffers B, C and D, high texture degrees correspond to the higher dispersion of energy barriers (Table 1). The difference between σ_W of the sample with Cu buffer and samples with buffers B–D is very high, which obviously shows as different MOKE domain images and magnetization relaxation $B(t)$ shape (Fig. 1). Contrary to samples B–D, for which magnetization reversal process occurs by growth of large cylindrical domains, high micromagnetic inhomogeneity of the sample A is depicted by a high nucleation rate of small domains. Barkhausen volumes V_B (Table 1), calculated with 5% of uncertainty, also show dependence on the magnetization reversal mechanism.

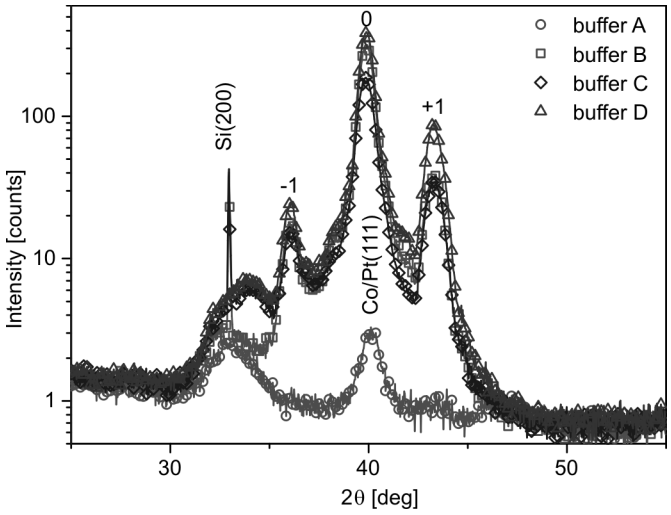

Fig. 7. X-ray diffraction θ–2θ profiles

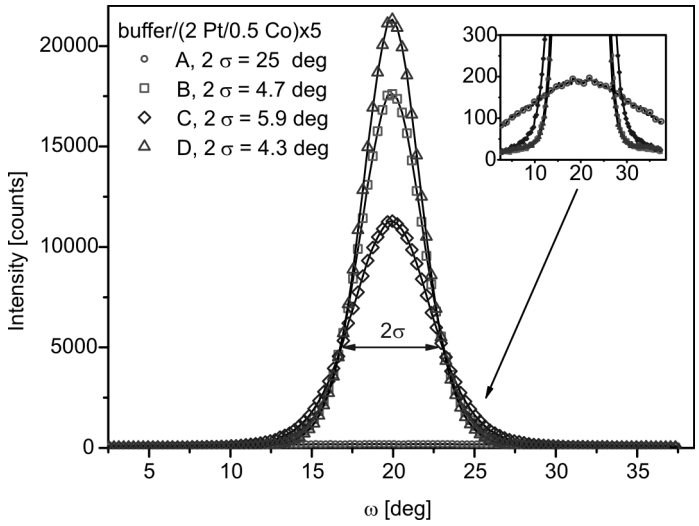

Fig. 8. Rocking curves (ω scans) of samples A, B, C and D at the Bragg position of (111) Co/Pt and corresponding peak half widths 2σ

The smallest V_B is observed for sample A with a high density of nucleation centres, while the highest V_B value is for sample C with the lowest σ_W energy dispersion, although this relationship is not distinctive as a correlation between σ_W and the texture degree. One must note that the surface morphology of sample A deposited on 10 nm Cu buffer with an asymmetric height distribution (Fig. 6) appear to be less regular in comparison to the samples with Ta/Cu buffers. We claim that the differences between samples with B, C, and D buffer types are quantitative only, with different texture

degree but well defined superlattice structure. On the contrary, the growth of Cu buffer (sample A) produces poor quality of a superlattice structure. We claim that existence of both (200) and (111) Cu crystallographic orientations [17] is related to disorder of the buffer structure of single Cu layer.

4. Conclusions

Magnetic properties, especially the domain pattern and magnetization reversal process, strongly depend on structural properties of ferromagnetic multilayers determined by growth on various textured buffers. High texture degree and Pt/Co interface waviness result in a higher inhomogeneity of micromagnetic properties and a non-uniform magnetization reversal process, with pinning centres, non-reversed remnants and increased coercivity. Such inhomogeneities give rise to irreversible remagnetization process. In the extreme case of high fluctuation of magnetic properties caused by improper growth of the seed buffer (for example 10 nm Cu on amorphous SiO_2), the saturation field should be high enough to provide uniform magnetization and overcome energy barrier blocking reversal of local pinning centres.

Thermally activated magnetization relaxations are very sensitive to the spatial dispersion of reversal energy barriers, thus analysis of the relaxation curves is a good tool to study quality of layers and multilayers with perpendicular magnetic anisotropy.

Acknowledgements

This work was supported by projects of Polish Ministry of Science and Higher Education and project of Research and Training Network (RTN) NANOMAG-LAB (No. 2004-003177).

References

[1] CARCIA P.F., MEINHOLDT A.D., SUNA A., Appl. Phys. Lett. 47, (1985) 178.
[2] DEN BROEDER F.J.A., KUIPER D., VAN DE MOSSELAER A.P., HOVING W., Phys. Rev. Lett. 60, (1988) 2769.
[3] CARCIA P.F., J. Appl. Phys 63, (1988) 5066.
[4] JEONG J-R., KIM Y-S., SHIN S-C., J. Appl. Phys, 85, (1999) 5762.
[5] MAAT S., TAKANO K., PARKIN S.S.P., FULLERTON E.E., Phys. Rev. Lett. 87, (2001) 087202.
[6] HELLWIG O., MAAT S., KORTRIGHT J.B., FULLERTON E.E., Phys. Rev. B 65, (2002) 144418.
[7] GARCIA F., CASALI G., AUFFRET S., RODMACQ B., DIENY B., J. Appl. Phys. 91, (2002) 6905.
[8] SORT J., RODMACQ B., AUFFRET S., DIENY B., Appl. Phys Lett. 83, (2003) 1800.
[9] VAN DIJKEN S., MORITZ J., COEY J.M.D., J. Appl. Phys. 97, (2005) 063907.
[10] SORT J., BALTZ V., GARCIA F., RODMACQ B., DIENY B., Phys. Rev B 71, (2005) 054411.
[11] KANAK J., STOBIECKI T., VAN DIJKEN S., IEEE Trans. Mag., 44 (2008), 238.
[12] ROMANENS F., PIZZINI S., YOKAICHIYA F., BONFIM M., PENNEC Y., CAMARERO J., VOGEL J., SORT J., GARCIA F., RODMAQ B., DIENY B., Phys. Rev. B 72, (2005) 134410.
[13] CZAPKIEWICZ M., VAN DIJKEN S., STOBIECKI T., RAK R., ZOLADZ M., MIETNIOWSKI P., Phys. Stat. Sol. (c) 3, (2006) 48.

[14] WIEBEL S., JAMET J.-P., VERNIER N., MOUGIN A., FERRÉ J., BALTZ V., RODMACQ B., DIENY B., J. Appl. Phys 100, (2006) 043912,.
[15] MALINOWSKI G., VAN DIJKEN S., CZAPKIEWICZ M., STOBIECKI T., Appl. Phys Lett. 90, (2007) 082501.
[16] CZAPKIEWICZ M., STOBIECKI T., VAN DIJKEN S., Phys. Rev. B, 77 (2008), 024416.
[17] WISNIOWSKI P., STOBIECKI T., KANAK J., REISS G., BRÜCKL H., J. Appl. Phys. 100 (2006) 013906.
[18] DAALDEROP G.H.O., KELLY P.J., SCHUURMANS M.F.H., Phys. Rev. B 42, (1990) 7270.
[19] WRONA J., STOBIECKI T., RAK R., CZAPKIEWICZ M., STOBIECKI F., UBA L., KORECKI J., SLEZAK T., WILGOCKA-SLEZAK J., ROTS M., Phys. Stat. Sol. (a) 196, (2003) 161.
[20] ZOLADZ M., KNAPPMANN S., OTTO M., RÖLL K., STOBIECKI T., Phys. Stat. Sol. (a) 189, (2002) 791.
[21] POMMIER J., MEYER P., PÉNISSARD G., FERRÉ J., BRUNO P., RENARD D., Phys. Rev. Lett. 65, (1990) 2054.
[22] LABRUNE M., ANDRIEU S., RIO F., BERNSTEIN P., J. Magn. Magn. Mater. 80, (1989) 211.
[23] FATUZZO E., Phys.Rev. 127, (1962) 1999.
[24] BRUNO P., BAYREUTHER G., BEAUVILLAIN P., CHAPPERT C., LUGERT G., RENARD D., RENARD J.P., SEIDEN J., J. Appl. Phys. 68, (1990) 5759.
[25] FERRÉ J., GROLIER V., MEYER P., LEMERLE S., MAZIEWSKI A., STEFANOWICZ E., TARASENKO S.V., TARASENKO V.V., KISIELEWSKI M., RENARD D., Phys. Rev. B 55, (1997) 15092.
[26] KISIELEWSKI M., MAZIEWSKI A., TEKIELAK M., FERRÉ J., LEMERLE S., MATHET V., CHAPPERT C., J. Magn. Magn. Mater, 260 (2003) 231–243.
[27] Meneghini C., MARET M., PARASOTE V., CADEVILLE M.C., HAZEMANN J.L., CORTES R., COLONNA S., Eur. Phys. J. B 7, (1999) 347.
[28] JANG H-J., CHOE S-B., SHIN S-C., J. Appl. Phys 93, (2003) 10143.

Received 30 April 2007
Revised 10 May 2007